The EMBO Journal vol.14 no.12 pp.2745–2759, 1995

The role of *Saccharomyces cerevisiae* type 2A phosphatase in the actin cytoskeleton and in entry into mitosis

Fong C.Lin and Kim T.Arndt

Cold Spring Harbor Laboratory, PO Box 100, Cold Spring Harbor, NY 11724, USA

We have prepared a temperature-sensitive *Saccharomyces cerevisiae* type 2A phosphatase (PP2A) mutant, *pph21-102*. At the restrictive temperature, the *pph21-102* cells arrested predominantly with small or aberrant buds, and their actin cytoskeleton and chitin deposition were abnormal. The involvement of PP2A in bud growth may be due to the role of PP2A in actin distribution during the cell cycle. Moreover, after a shift to the non-permissive temperature, the *pph21-102* cells were blocked in G2 and had low activity of Clb2–Cdc28 kinase. Expression of Clb2 from the *S.cerevisiae ADH* promoter in *pph21-102* cells was able to partially bypass the G2 arrest in the first cell cycle, but was not able to stimulate passage through a second mitosis. These cells had higher total amounts of Clb2–Cdc28 kinase activity, but the Clb2-normalized specific activity was lower in the *pph21-102* cells compared with wild-type cells. Unlike wild-type strains, a PP2A-deficient strain was sensitive to the loss of *MIH1*, which is a homolog of the *Schizosaccharomyces pombe* mitotic inducer *cdc25*$^+$. Furthermore, the *cdc28F19* mutation cured the synthetic defects of a PP2A-deficient strain containing a deletion of *MIH1*. These results suggest that PP2A is required during G2 for the activation of Clb–Cdc28 kinase complexes for progression into mitosis.

Key words: actin/Cdc28/Clb2/MIH1/PP2A

Introduction

In *Saccharomyces cerevisiae*, *PPH21* and *PPH22*, both encoding catalytic subunits of serine/threonine protein phosphatase 2A, have been identified (Sneddon *et al.*, 1990; Ronne *et al.*, 1991; Sutton *et al.*, 1991a) and implicated in bud morphogenesis (Ronne *et al.*, 1991). Bud emergence and growth in *S.cerevisiae* cells are coupled to a sequential reorganization of the actin cytoskeleton during the cell cycle (Chant and Pringle, 1991; Drubin, 1991). The redistribution of actin patches through the cell cycle may be regulated by cyclins and Cdc28, which is a homolog of the *Schizosaccharomyces pombe* cdc2 kinase (Lew and Reed, 1993). In eukaryotic cells, the initiation of mitosis is known to be controlled by a kinase complex of cyclin B and cdc2 (Nurse, 1990; Solomon, 1993). In *S.pombe* or *Xenopus*, a critical pathway necessary to activate cyclin B–cdc2 kinase activity is the dephosphorylation of tyrosine 15 of cdc2 (Dunphy and Newport, 1989; Gould and Nurse, 1989; Solomon *et al.*, 1990). This activating modification is mediated by a mitotic inducer, the cdc25 tyrosine phosphatase (Dunphy and Kumagai, 1991; Gautier *et al.*, 1991; Strausfeld *et al.*, 1991), which counteracts the inhibitory phosphorylation of the same tyrosine by the wee1 and mik1 kinases (Russell and Nurse, 1987; Lundgren *et al.*, 1991). In *S.pombe*, genetic analysis has suggested that PP2A, like wee1, inhibits entry into mitosis (Kinoshita *et al.*, 1993). Kumagai and Dunphy (1992) have reported that PP2A might be the phosphatase in *Xenopus* extracts that inhibits the activity of cdc25. Moreover, a purified enzyme from immature oocytes, named INH, was found to be a form of PP2A which might inactivate the cdc2 kinase (Lee *et al.*, 1991, 1994). These results suggest that, under certain conditions in these organisms, PP2A may be able to negatively regulate the activity of cyclin B–cdc2 complexes, possibly through multiple pathways.

The Cdc28 kinase in *S.cerevisiae* has been shown to play a key role in mitotic initiation (Piggott *et al.*, 1982; Reed and Wittenberg, 1990; Surana *et al.*, 1991), and its association with B-type cyclins encoded by *CLB1*, *CLB2*, *CLB3* and *CLB4* is necessary for entry into mitosis (Ghiara *et al.*, 1991; Surana *et al.*, 1991; Fitch *et al.*, 1992; Richardson *et al.*, 1992). Among these cyclins, Clb2 is considered the major mitotic cyclin, and the activation of Clb2–Cdc28 complexes is important for the onset of mitosis (Surana *et al.*, 1991; Fitch *et al.*, 1992; Richardson *et al.*, 1992). There is some evidence that the Cdc28 kinase is regulated for mitosis by *MIH1* and *SWE1*, the budding yeast homologs of *cdc25*$^+$ and *wee1*$^+$, respectively (Russell *et al.*, 1989; Booher *et al.*, 1993). Similar to the counteracting functions of cdc25 and wee1, the deletion of *MIH1* causes a mitotic delay which can be abolished by the loss of *SWE1* (Russell *et al.*, 1989; Booher *et al.*, 1993). However, unlike cdc2 of *S.pombe*, replacement of the conserved tyrosine 19 in Cdc28 by a phenylalanine resulted in very little change in the mitotic activation of the Clb–Cdc28 kinase (Amon *et al.*, 1992; Sorger and Murray, 1992). These findings could be explained by the presence of an additional, as yet unidentified, pathway that is crucial for the mitotic activation of Clb–Cdc28 kinase complexes.

Here we describe two cell cycle defects resulting from a defect in PP2A in budding yeast. One defect is that the cells arrest with small or aberrant buds, where the actin distribution is disorganized and the chitin deposition is delocalized. We suggest that without the function of PP2A, the cells are unable to maintain their proper actin cytoskeleton so that normal bud growth is prevented. The other defect is that the arrested cells are blocked in G2, where the chromosomal DNA is replicated but the nuclei are not divided and the mitotic spindles are not able to form or are not able to extend. Genetic and biochemical studies suggest that PP2A is required to activate the kinase activity of Clb–Cdc28 complexes for the advancement from G2 into mitosis.

Results

A temperature-sensitive pph21-102 mutant

PPH22, a gene encoding a catalytic subunit of PP2A in *S.cerevisiae*, has been isolated previously in our laboratory (Sutton *et al.*, 1991a). Later, we identified a second gene, *PPH21*, which encodes a PP2A catalytic subunit (see Materials and methods). The deletion of either *PPH21* or *PPH22* alone caused no detectable effect, but the deletion of both genes resulted in a slow growth defect and a leaky temperature-sensitive phenotype at 37°C (data not shown). Only the deletion of *PPH21*, *PPH22* and a PP2A-related gene, *PPH3*, was lethal. These results agree with the findings of Ronne *et al.* (1991).

To investigate whether PP2A is involved in cell cycle events, we prepared a temperature-sensitive PP2A mutant. The amino acid residue altered in the *sit4-102* temperature-sensitive allele is conserved between Sit4, a type 2A-related phosphatase, and all known type 2A protein phosphatases (Figure 1A; Sutton *et al.*, 1991b). We made the equivalent alteration in Pph21, where the glutamate at position 102 was replaced by a lysine (Figure 1A and see Materials and methods). The mutated gene on a centromere plasmid was introduced into a *Δpph21 Δpph22 Δpph3* strain by plasmid shuffling, and the resulting strain is termed a *pph21-102* mutant. At 24°C, the growth rate of the *Δpph21 Δpph22 Δpph3* strain with the wild-type *PPH21* gene on a centromere plasmid was similar to that of the wild-type strain, but the *pph21-102* mutant grew at a slightly slower rate than the wild-type strain (Figure 1B). When incubated at 36°C, the *pph21-102* mutant was not able to grow (Figure 1B). This temperature-sensitive phenotype can be rescued by transformation with either the *PPH21* or *PPH22* gene on a centromere plasmid (data not shown), confirming that the mutation in *PPH21* is responsible for the temperature-sensitive phenotype. These findings also indicate that the *pph21-102* mutation is recessive.

We examined whether the non-permissive temperature causes cell death for the *pph21-102* mutant. The viability of the *pph21-102* cells did not decrease during a 3 h incubation at 36°C. Therefore, the shift to the non-permissive temperature results in the arrest of cell division rather than cell death. Moreover, at 36°C the arrested *pph21-102* cells continued to grow. During the 3 h incubation at 36°C, the *pph21-102* cells increased in cell size by 20–25%, while the wild-type cells did not increase in size (also see Figure 3). Furthermore, after a shift to the non-permissive temperature, *pph21-102* and wild-type cells incorporated similar amounts of [^{35}S]methionine (data not shown). These results suggest that the arrest of *pph21-102* cells at the non-permissive temperature is not due to cell death or to an arrest of cell growth.

pph21-102 cells have a defect in bud growth

To characterize the effect due to the loss of PP2A function, *pph21-102* and wild-type (where *PPH21*, *PPH22* and *PPH3* are intact) cells were grown exponentially at 24°C and then shifted to 36°C for 3 h. At the permissive temperature there was no significant difference in the morphology between wild-type and *pph21-102* cells. However, at 36°C the *pph21-102* cells arrested with a heterogeneous bud morphology. Photographs of representative

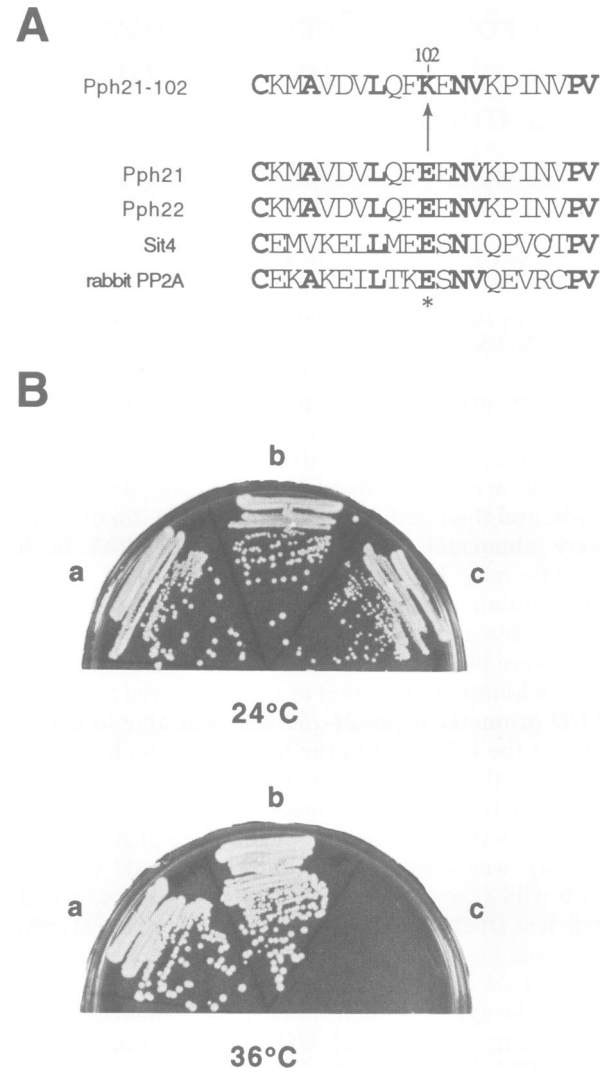

a, Wild Type
b, *Δpph21 Δpph22 Δpph3 [PPH21/TRP/CEN]*
c, *Δpph21 Δpph22 Δpph3 [PPH21-102/TRP/CEN]*

Fig. 1. A temperature-sensitive *pph21-102* mutant. (**A**) A single amino acid substitution in the Pph21-102 protein. The glutamate residue (indicated by the asterisk) is conserved between PP2A and Sit4, and is replaced by the lysine at position 102 of Pph21-102. (**B**) Photographs of (a) wild-type (W303), (b) *Δpph21 Δpph22 Δpph3* mutant strain carrying *PPH21/TRP1/CEN* (CY1678) and (c) *Δpph21 Δpph22 Δpph3* strain carrying *pph21-102/TRP1/CEN* (CY3006), streaked to single colonies on YEPD plates and incubated at either 24 (top) or 36°C (bottom) for 3 or 2 days, respectively.

pph21-102 cells having each phenotype are shown in Figure 2A, and the various cell morphology phenotypes of the wild-type and the *pph21-102* mutant at different temperatures are summarized in Figure 2B. Six different bud phenotypes of the arrested *pph21-102* cells were categorized (Figure 2A and B): unbudded (Figure 2A, plate a), small buds (Figure 2A, plates b and c), hook-like buds (Figure 2A, plates d–g), tube-like buds (Figure 2A, plates h and i), large angular buds (Figure 2A, plates j and k) and large buds (Figure 2A, plate l). Approximately 40% of the cells had a small bud with an apparent normal morphology. The hook-like buds were variable in both appearance and size. The large angular buds were often

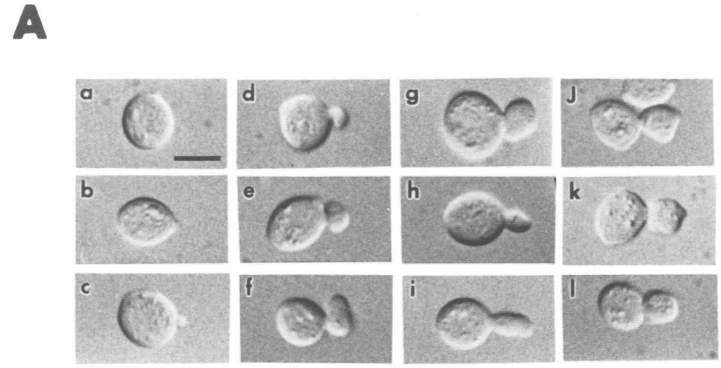

B

	Temperature	multibudded	elongated buds	% cells with mitotic spindle
Wild Type	24°C	35 25 41 0 0	2 19 7 9	35
Wild Type	36°C	35 33 32 0 0	0 14 6 8	28
Δpph21 Δpph22	24°C	18 28 49 4 1	10 22 4 10	36
pph21-102	24°C	34 25 42 0 0	2 25 3 9	37
pph21-102	36°C	16 42 18 6 9 10	3 10 <1 <1	11

Fig. 2. Arrested *pph21-102* cells had a defect in bud growth. (**A**) Photographs showing morphologies of sonicated haploid *pph21-102* cells (CY3007) incubated at 36°C for 3 h. A variety of arrested bud-shaped phenotypes were seen and categorized into six different groups (see also B): a, unbudded; b and c, small buds; d–g, hook-like buds; h and i, tube-like buds; j and k, large angular buds; l, large bud. Bar, 4 μm. (**B**) Wild-type (W303), *Δpph21 Δpph22* (CY1145) and *pph21-102* (CY3007) strains were grown in YEPD medium at 24°C, shifted to 36°C for 3 h and samples from both 24 and 36°C were stained with DAPI and tubulin-specific antibody. For each sample, at least 300 cells were counted. On the left side, the percentages of cells that were unbudded, small-budded or large-budded are indicated. For the arrested *pph21-102* cells at 36°C, six different bud shapes were categorized. On the right side, further characterization of the large budded cells was performed. The percentages of total cells with large buds with a particular nuclear morphology (upper panel) and microtubule (lower panel) morphology, and the percentages of total cells with mitotic spindles are indicated. Four types of cell were scored: an undivided nucleus with a single microtubule organizing center in the mother cell, an undivided nucleus with a short spindle in the mother cell, an undivided but stretched nucleus with an elongated spindle in the bud neck, and a divided nucleus with an elongated spindle extending from the mother into the bud.

bumpy, giving a square, trapezoid or pentagon shape. In summary, the variety of arrested bud morphologies suggests that there is a defect in bud growth for the *pph21-102* cells at the non-permissive temperature. The deletion of *PPH22* and *PPH21* was synthetically lethal in combination with a deletion of *BEM2* (data not shown), suggesting that PP2A is involved in bud morphogenesis. This synthetic lethal phenotype could be suppressed by a centromere plasmid carrying *PPH22*, *PPH21* or *BEM2*. *BEM2* is involved in polarity establishment and bud emergence (Bender and Pringle, 1991).

To investigate further the role of PP2A in bud morphology, we wanted to shift synchronized *pph21-102* cells to the non-permissive temperature. We could not use nocodazole to synchronize the cells because the *pph21-102* cells lost viability during the nocodazole treatment. We also tried α factor arrest and release. The *pph21-102* cells were not able to recover from the α factor arrest if they were immediately shifted to the non-permissive temperature. However, if the *pph21-102* cells were shifted to 36°C at various times after recovery from the α factor arrest (after they initiated a bud), the synchronized cells arrested with similar phenotypes as the asynchronous *pph21-102* culture (data not shown).

pph21-102 cells have an alteration in the actin cytoskeleton and chitin deposition

The frequent occurrence of both small and aberrant buds in the arrested *pph21-102* cells could be due to a defect in bud growth. In *S.cerevisiae*, bud emergence and bud growth seem to depend upon a rearrangement of the actin cytoskeleton during the cell cycle (Adams and Pringle, 1984; Kilmartin and Adams, 1984). Therefore we examined whether an alteration in the actin cytoskeleton occurs in the *pph21-102* cells after a shift to the restrictive temperature.

The cell cycle-dependent pattern of actin assembly in wild-type cells is shown in Figure 3A. Actin occurs in two forms: cytoplasmic cables and cortical patches. During the cell cycle, the actin patches were predominantly distributed at the site of bud emergence (Figure 3A, plate b), in the growing bud (Figure 3A, plates c–e) and at the

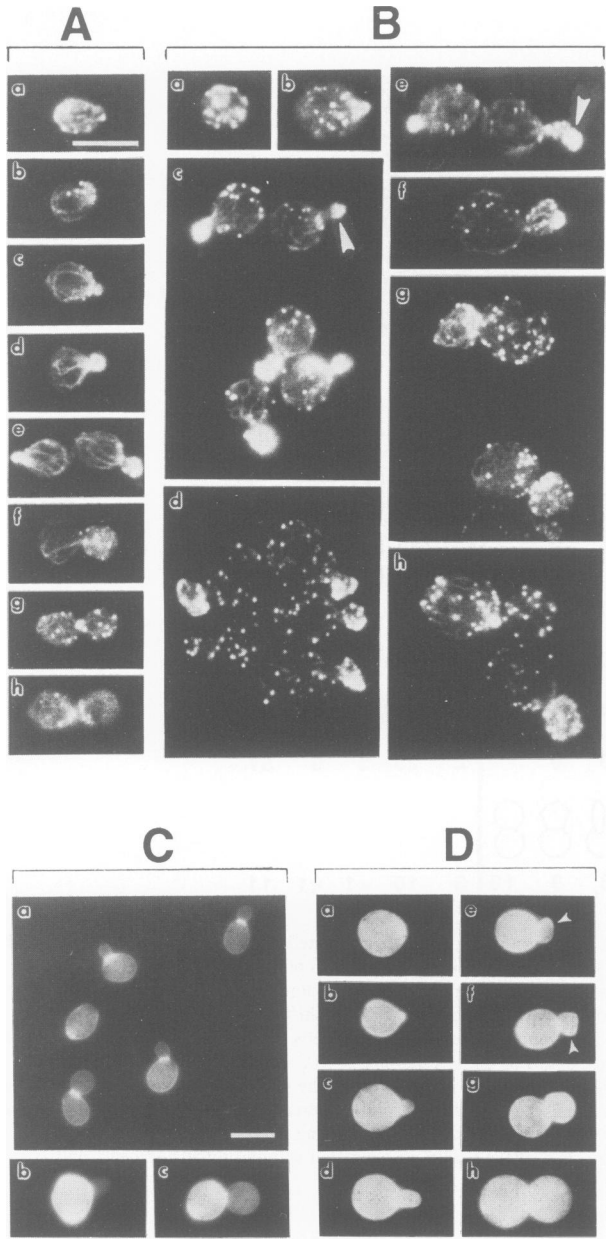

Fig. 3. Altered actin and chitin localization in *pph21-102* cells. Wild-type (W303) and *pph21-102* (CY3007) cells were grown to log phase in YEPD medium at 24°C, and then incubated at 36°C for 3 h. The cells were fixed, stained with rhodamine phalloidin (**A** and **B**) or Calcoflour (**C** and **D**), and visualized with epifluorescence microscopy. (A) The sequential distribution of actin (plates a–h) in wild-type cells during the cell cycle. Bar, 4 μm (A and B). (B) Altered actin distribution in *pph21-102* cells with different bud shapes (plates a–h). The photograph shown in plate c was focused for the cytoplasmic actin cables of the mother cell, and in plate d was focused for the cortical actin patches of the bud. Arrowheads in plates c and e indicate tube-like buds. (C) Chitin distribution in wild-type cells. Bar, 4 μm (C and D). (D) Delocalization of chitin deposition in *pph21-102* cells. Arrowheads in plates e and f indicate more intensely staining regions in the buds.

neck during cytokinesis (Figure 3A, plate h). Actin cables were mostly parallel to the mother-bud axis and were seen mostly in the mother cells (Figure 3A, plates b–f). Shortly before cytokinesis, a few actin patches were seen in the mother, and the cables appeared in the bud (Figure 3A, plate g). After septation, the distribution of cortical actin patches and cytoplasmic actin cables became randomized in the unbudded G1 cells (Figure 3A, plate a).

The *pph21-102* mutant growing at 24°C had the same actin distribution as the wild-type cells (data not shown). However, following a shift from 24 to 36°C, several alterations in actin localization occurred in the *pph21-102* cells compared with the isogenic wild-type cells. In the budded *pph21-102* cells, the actin patches maintained a polarized distribution but many were scattered throughout the mother cell (Figure 3B, plates b–e), where the distribution of actin cables was somewhat disorganized (Figure 3B, plates c and d). Unlike in wild-type buds, the actin patches in the defective *pph21-102* buds were unevenly distributed and sometimes concentrated at the corner of the bud (Figure 3B, plates d and f). For the cells with a large angular bud, a cluster of patches accumulated only on the mother side or the bud side of the neck (Figure 3B, plates g and h). Therefore, a defect in PP2A activity causes alterations in the actin cytoskeleton.

In actin mutants that have an altered distribution of actin, the chitin deposition is also delocalized (Drubin *et al.*, 1993). We then examined the chitin distribution. In wild-type cells, chitin was observed in a ring at the neck of the emerging bud (Figure 3C, plate a). The mother cells with several chitin rings stained much brighter than the buds (Figure 3C, plates b and c). By contrast, in the arrested *pph21-102* cells the chitin was distributed diffusely over the entire cell surface of both the mother and the bud (Figure 3D), leading to an impression that the bud was stained as brightly as the mother cell. The staining of the chitin ring was still recognizable, but was not as clear as in the wild-type cells (Figure 3D, plates c–h). Some of the *pph21-102* cells with a hook-like bud or bumpy bud had abnormally located patches of chitin (Figure 3D, plates e and f, arrowheads).

pph21-102 cells have a G2 block and PP2A-deficient cells had a G2 delay

When the *pph21-102* mutant was shifted to the non-permissive temperature, ~85% of the cells were budded (Figure 2B) and 85% of the cells had a 2N DNA content (Figure 4A), suggesting that the budded cells had completed DNA replication. Most of these cells (85% of total cells) possessed a single microtubule organizing center located at the bud-proximal side of the nucleus, sometimes with a bundle of microtubules extending towards the bud (Figure 4B and C, plates a and b). Based on light microscopy, we cannot ascertain if the spindle pole body is duplicated within the microtubule organizing center. In contrast to 28% of wild-type cells, only 11% of the arrested *pph21-102* cells had mitotic spindles. These spindles were short and only extended across the unstretched nucleus next to the neck (Figure 4B and C, plates c and d), which is characteristic of cells in G2 (Byers, 1981). Even in the cells where the nucleus was located in the neck, there was only a short spindle (Figure 4B and C, plate e). Therefore, most of the *pph21-102* cells arrested with a bud, a 2N DNA content, an undivided nucleus and either a single microtubule organizing center (74% of all cells) or an unextended mitotic spindle (11% of all cells).

Additional evidence to support a requirement for PP2A during G2 is from a phenotypic characterization of a

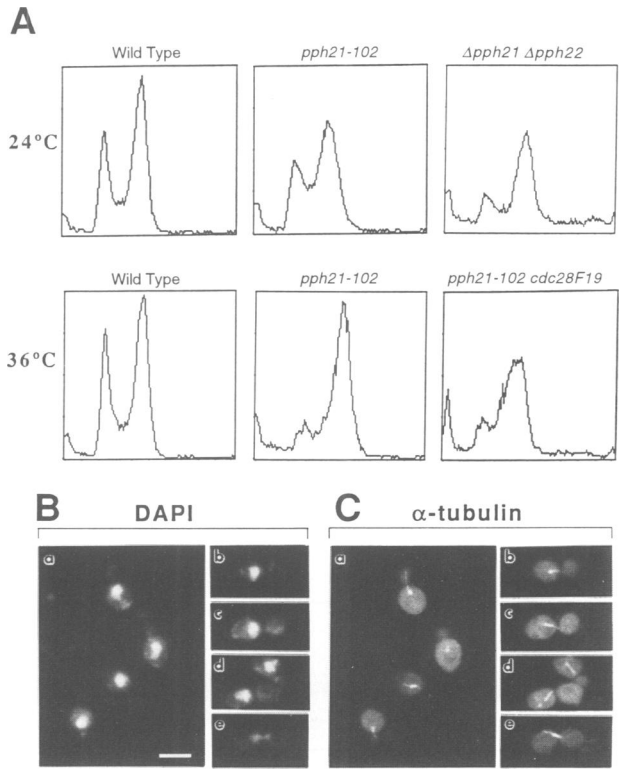

Fig. 4. *pph21-102* cells arrested with a G2 block. (**A**) Wild-type (W303), *pph21-102* (CY3007), *pph21-102 cdc28F19* (CY3008) and *Δpph22 Δpph21* (CY1145) cells were grown exponentially in YEPD medium at 24°C, and shifted to 36°C for 3 h. DNA content of propidium iodide-stained cells was determined by flow cytometry (see Materials and methods). (**B** and **C**) Fluorescent microscopy of the arrested *pph21-102* cells. Asynchronous cultures of the *pph21-102* mutant (CY3007) were grown in YEPD medium at 24°C and shifted to 36°C for 3 h. Cells were harvested, fixed in formaldehyde and stained with DAPI and tubulin-specific antibody. Photographs of different cells with nuclei (B) and the corresponding microtubules and spindles (C) are shown. Bar, 4 μm.

Δpph21 Δpph22 mutant. At 24°C, ~83% of the *Δpph21 Δpph22* cells in a log phase culture were budded. Flow cytometry analysis (Figure 4A) showed that 80–85% of cells had a 2N DNA content, suggesting that most of the budded cells completed DNA replication. Moreover, large budded cells were the predominant form of budded cell (Figure 2B). Although the percentage of cells with mitotic spindles showed little difference between the wild-type and *Δpph21 Δpph22* cultures (Figure 2B), the percentage of large budded cells with a single microtubule organizing center increased from 2% for a wild-type culture to 10% for a *Δpph21 Δpph22* culture (Figure 2B). These observations suggest that the deletion of both *PPH21* and *PPH22* results in a G2 delay at 24°C.

When released from a hydroxyurea arrest and shifted to the non-permissive temperature, pph21-102 cells fail to enter mitosis

The results shown above suggest a role for PP2A in bud morphogenesis and in progression through G2. It has been suggested that some cell cycle events, like budding and nuclear division, can be independent of each other (Pringle and Hartwell, 1981). We asked whether the requirement of PP2A for progression from G2 into M phase can be separated from its role in normal bud growth. If PP2A is a positive factor for progression from G2 into M phase, then a non-functional PP2A should prevent large-budded G2 cells from entering mitosis. To test this hypothesis, we first synchronized wild-type and *pph21-102* cells with hydroxyurea at 24°C for 3 h, which gave an S phase arrest where ⩾80% of cells were large budded. Neither strain lost viability during the 3 h incubation with hydroxyurea (94% of wild-type cells and 92% of *pph21-102* cells were viable). Subsequently, the arrested cells were filtered, washed, resuspended in fresh medium, shifted to 37°C and sampled every 15 min.

The *pph21-102* cells and wild-type cells replicated their DNA with similar kinetics (Figure 5A). The wild-type cells progressed into mitosis, passed G1 phase, budded and replicated their DNA again (Figure 5B and C). Moreover, the nucleus divided, the mitotic spindle extended and the percentage of cells with mitotic spindles changed from 67% at 0 min, to 40% at 60 min, to 53% at 120 min. In contrast, by the 120 min time point the *pph21-102* cells still had mainly a 2N DNA content (Figure 5A), were still large-budded and their cell density and percentage of budded cells remained essentially constant (Figure 5B and C). Furthermore, the nucleus failed to migrate, the mitotic spindle failed to extend and the percentage of cells with mitotic spindles actually decreased from 54% at 0 min, to 17% at 60 min, to 10% at 120 min. As a result, most of the cells arrested with a large bud and a single microtubule organizing center, possibly due to collapse of the spindles. This requirement for PP2A to maintain the mitotic spindles may be related to the sensitivity of *pph21-102* cells to nocodazole. In summary, even after a large bud is formed, the *pph21-102* cells replicate their DNA but are unable to form or to elongate mitotic spindles, and fail to advance from G2 into mitosis at the non-permissive temperature. These defects due to the absence of PP2A function resemble the terminal phenotype seen for the loss of Clb1, Clb2, Clb3 and Clb4 function (Amon *et al.*, 1993).

PP2A is required for the activation of the Clb–Cdc28 kinase

In *S.cerevisiae*, activation of the Clb–Cdc28 kinase is necessary for the cells to enter mitosis. Therefore, we determined whether after a shift to the non-permissive temperature, the synchronized large-budded *pph21-102* cells have a loss of Clb–Cdc28 kinase activity. Wild-type and *pph21-102* cells were released from a hydroxyurea arrest and shifted to 37°C as described above. Then, the Clb–Cdc28 kinase activity was assayed at various times up to 2 h, by which time the wild-type cells entered another cell cycle (Figure 5A). Because Clb2 is the most important mitotic cyclin (see Introduction), we monitored Clb2-associated kinase activity using Clb2 tagged with a triple-HA epitope (see Materials and methods).

For the wild-type cells, the Clb2-associated kinase activity towards histone H1 increased and was cell cycle-dependent (Figure 6A and D). By contrast, the kinase activity for the *pph21-102* cells was only half that of the wild-type cells at the 0 min time point, and decreased to very low levels after incubation at 37°C (Figure 6A and D). The levels of Clb2 and Cdc28 proteins in the immunoprecipitates from both wild-type and mutant cells

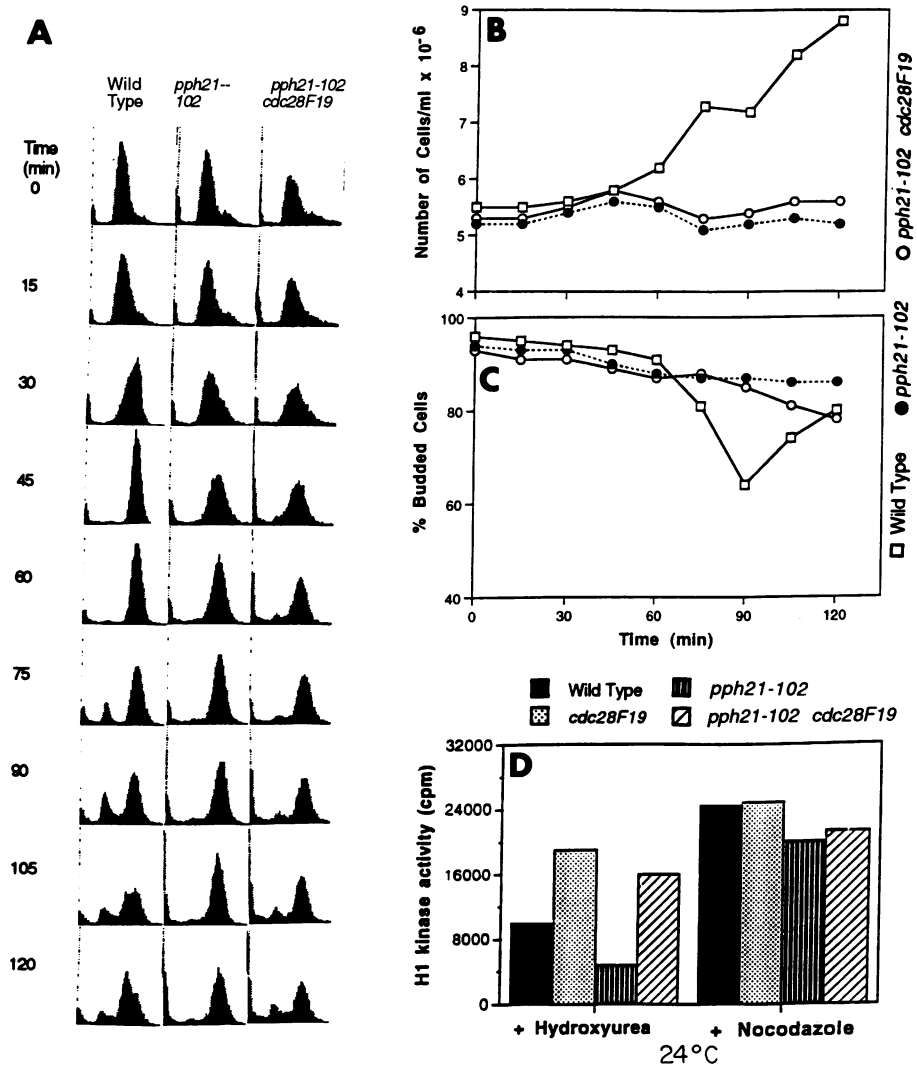

Fig. 5. Progression from G2 into mitosis requires PP2A function. A *pph21-102* mutant (CY3087; ●), a *pph21-102 cdc28F19* mutant (CY3089; ○) and a wild-type strain (CY2999; □), all containing *CLB2-HA*, were grown in YEPD medium to log phase and then synchronized in S phase by hydroxyurea treatment at 24°C for 3 h. Next, the cells were filtered, washed, resuspended into fresh YEPD medium and shifted to 37°C. Samples were taken every 15 min for 120 min to determine DNA content (**A**), cell density (**B**) and budding index (**C**). (**D**) Comparison of the Clb2-associated kinase activity in hydroxyurea- or nocodazole-arrested cells. A wild-type strain (CY2999), a *cdc28F19* mutant (CY3256), a *pph21-102* mutant (CY3087) and a *pph21-102 cdc28F19* mutant (CY3089), all containing *CLB2-HA*, were grown exponentially at 24°C in YEPD medium and synchronized either in S phase by adding hydroxyurea (0.2 M) or in M phase by adding nocodazole (15 μg/ml). After 3 h the cells were harvested. Extracts were prepared and Clb2-associated kinase activity was determined as described in Materials and methods. The graphs are the average of two independent experiments.

decreased with similar kinetics (Figure 6D), but the levels of these proteins from the wild-type cells were moderately higher than those from the *pph21-102* cells (Figure 6B and D). At the permissive temperature, the specific activity of the Clb2–Cdc28 kinase from the *pph21-102* cells was ~50% of that from the wild-type cells (0 min time point in Figure 6C). After the shift to 37°C, the specific activity of the Clb2–Cdc28 kinase, normalized by the levels of either Clb2 protein (Figure 6C) or Cdc28 protein (data not shown) from the wild-type cells, increased while the specific activity for the *pph21-102* cells decreased. A possible explanation for these results is that PP2A may have two effects: one on the intrinsic kinase activity of Clb2–Cdc28 complexes (seen as a decrease in the specific activity) and another on *CLB2* expression (seen as a modest decrease in Clb2 levels).

We therefore monitored the level of *CLB2* transcripts for cells released from a hydroxyurea arrest and shifted to 37°C. The level of *CLB2* RNA in the wild-type cells was periodic and at a somewhat higher level than that in *pph21-102* cells (data not shown). The lower levels of *CLB2* expression in the *pph21-102* mutant might be due to the proposed positive feedback loop where *CLB2* transcription requires Clb-associated kinase activity (Amon *et al.*, 1993). Unlike *CLB2* RNA, the levels of *CDC28* RNA were similar between the wild-type and *pph21-102* cells (data not shown). In addition, we monitored the levels of *CLN2* RNA because inactivation of the Clb2-associated kinase due to a lack of PP2A function should result in the inability to repress *CLN2* transcription (Amon *et al.*, 1993). Indeed, *CLN2* RNA levels increased after the *pph21-102* cells were shifted to 37°C (data not shown), during which time their Clb2–Cdc28 kinase activities correspondingly decreased

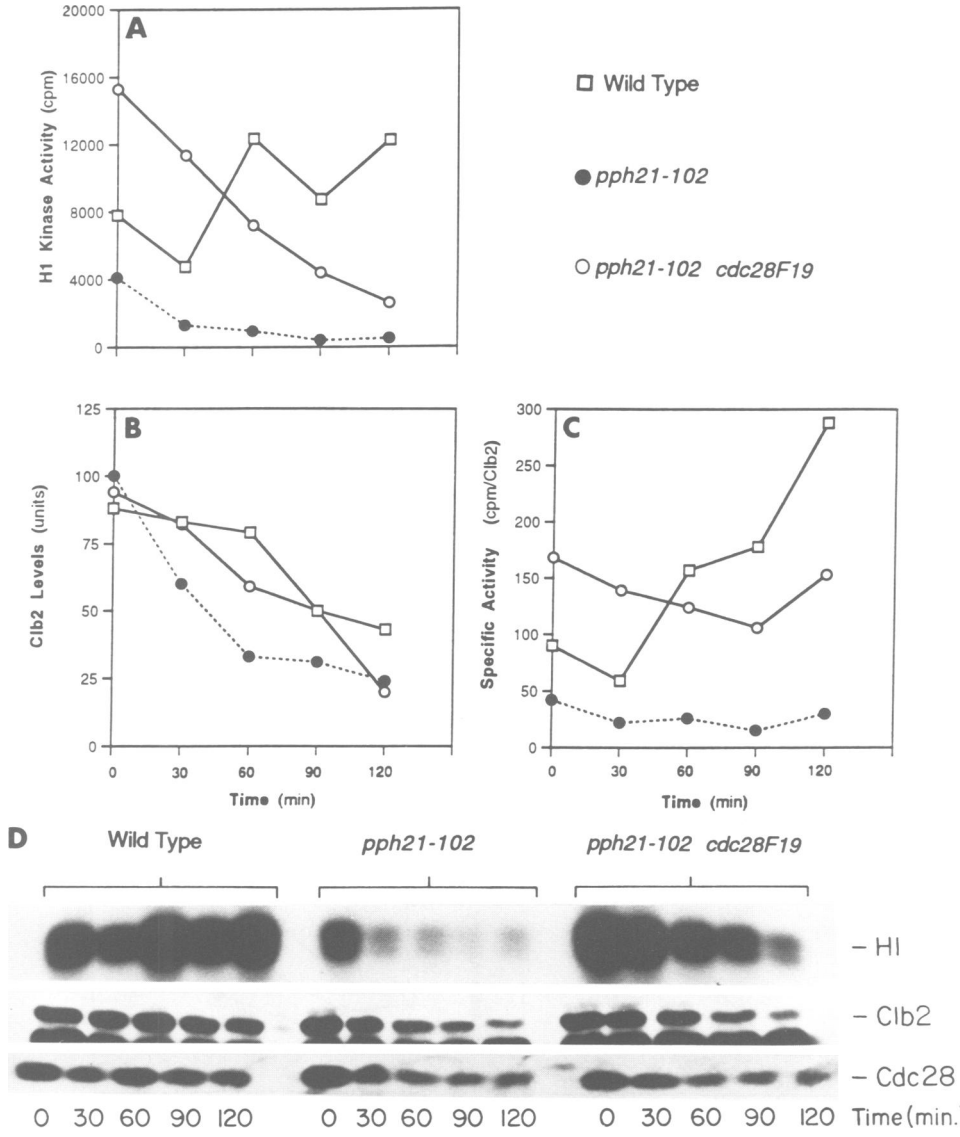

Fig. 6. PP2A is required for the activity of Clb2–Cdc28 kinase complexes. A wild-type strain (CY2999, □), a *pph21-102* mutant (CY3087, ●) and a *pph21-102 cdc28F19* mutant (CY3089, ○), all containing *CLB2-HA*, were arrested with hydroxyurea, released and then shifted to 37°C as described in the legend to Figure 5. Samples were taken every 30 min for 120 min to analyze Clb2-associated histone H1 kinase activity (**A** and **D**), the amounts of Clb2 (**B** and D), and the amounts of Cdc28 (D). The Clb2-normalized specific activity (the H1 kinase activity in c.p.m./arbitrary units of Clb2 protein) is shown in (**C**). Western blot of 12CA5 immunoprecipitates probed with 12CA5 monoclonal antibody for Clb2 or anti-Cdc28 antiserum for Cdc28 protein (D). The methods of quantitation are described in Materials and methods. The graphs are the average of two independent experiments and the photographs show only one of the experiments.

(Figure 6). This increase in *CLN2* RNA levels in the *pph21-102* cells provides evidence that Clb–Cdc28 kinase activity is defective *in vivo* in PP2A-deficient cells.

We also determined whether the expression of *CLB2* coding sequences from heterologous promoters would allow the *pph21-102* cells to enter mitosis at the non-permissive temperature. At 24°C, expression of Clb2 from either the *S.pombe ADH* (lower level) or the *S.cerevisiae ADH* (higher level) promoter had no significant effect on the growth rate of either wild-type or *pph21-102* cells. After release from a hydroxyurea arrest followed by a shift to 37°C, 5 (0 h), 14 (after 2 h) and 16% (after 4 h) of *pph21-102* cells expressing *CLB2* from the native promoter were unbudded. In contrast, 7 (0 h), 26 (after 2 h) and 17% (after 4 h) of the *pph21-102* cells expressing *CLB2* from the *S.cerevisiae ADH* promoter were unbudded. Therefore, the expression of Clb2 from the *S.cerevisiae ADH* promoter allows some cells to pass the first mitosis (at the 2 h time point), but is not able to stimulate passage through second mitosis (at the 4 h time point). We also analyzed the Clb2 levels and Clb2-associated kinase activity. The *pph21-102* cells expressing *CLB2* from the *S.pombe ADH* promoter accumulated higher levels of Clb2 protein than the wild-type cells expressing *CLB2* from the same promoter (Figure 7B). However, the *pph21-102* cells had both lower total Clb2–Cdc28 kinase activity and lower specific Clb2–Cdc28 kinase activity compared with the wild-type cells (Figure 7A and C). Similar effects also occurred in cells expressing *CLB2* from the *S.cerevisiae ADH* promoter (Figure 7D and F), except that the levels of Clb2 protein and total kinase activity were several-fold higher (compare Figure 7B and E). However, even when Clb2 is expressed from either heterologous promoter, the Clb2–Cdc28 complexes had lower specific activity in the

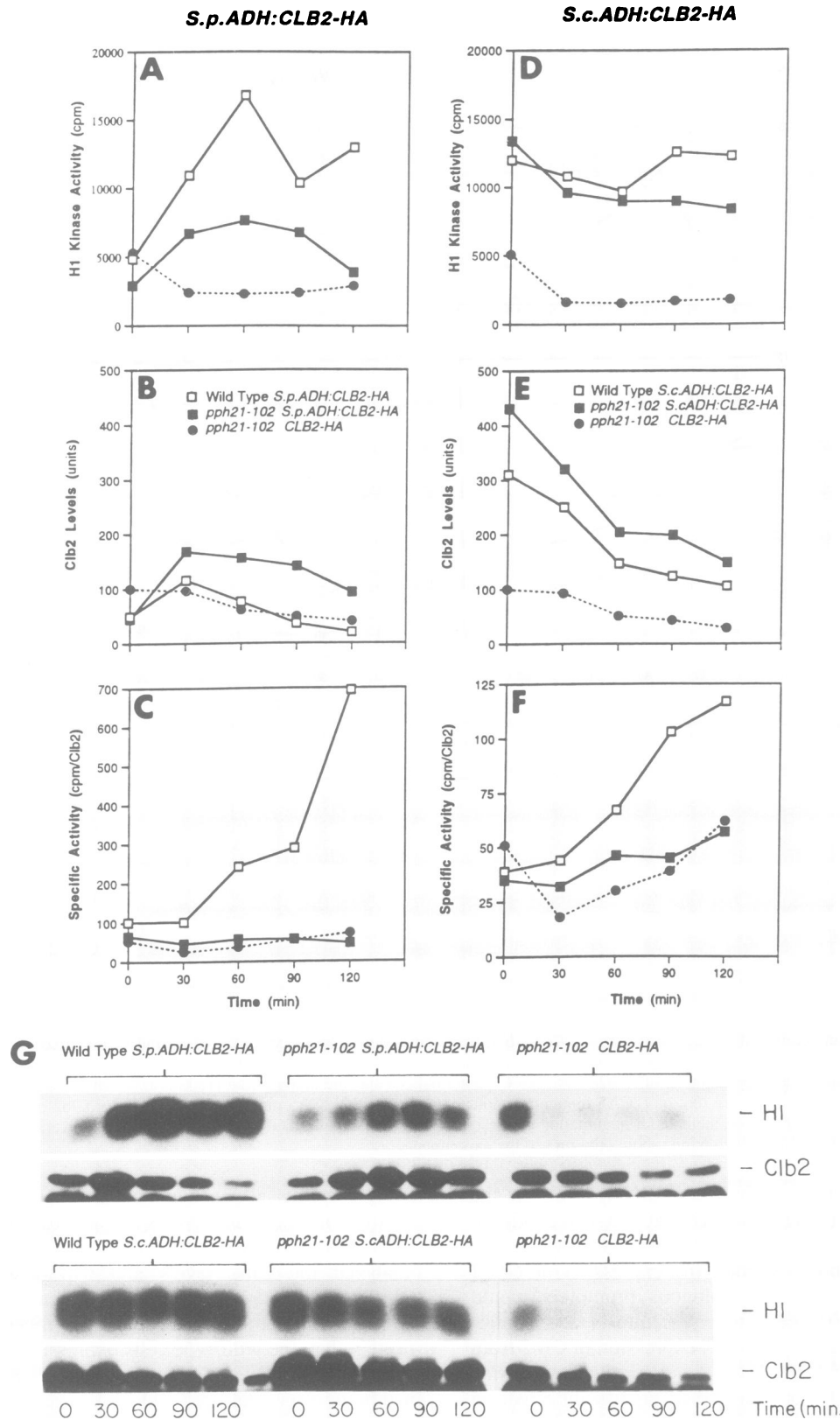

Fig. 7. Expression of *CLB2* from heterologous promoters does not cure the defect in Clb2–Cdc28 kinase activity in *pph21-102* cells. The following strains were used: for the left side, a *S.pombe ADH:CLB2-HA* strain (CY4279, □), a *S.pombe ADH:CLB2-HA pph21-102* mutant (CY4280, ■) and a *S.pombe ADH/YCp50 CLB2-HA pph21-102* mutant (CY4281, ●); for the right side, a *S.cerevisiae ADH:CLB2-HA* strain (CY4294, □), a *S.cerevisiae ADH:CLB2-HA pph21-102* mutant (CY4296, ■) and a *S.cerevisiae ADH/YCp50 CLB2-HA pph21-102* mutant (CY4299, ●). Cells were arrested with hydroxyurea, released and then shifted to 37°C as described in the legend to Figure 5, except that synthetic complete minus uracil medium was used to maintain plasmid selection. Samples were taken at 30 min intervals up to 120 min. Clb2-associated histone H1 kinase (**A**, **D** and **G**), Clb2 protein levels (**B**, **E** and **G**) and the specific activity (**C** and **F**, the H1 kinase activity in c.p.m./arbitrary units of Clb2 protein) are shown. For each experiment, the levels of Clb2 in the *pph21-102* strain (●) at the 0 time point were assigned to 100 U. The graphs are the average of two independent experiments and the photographs show only one of the experiments.

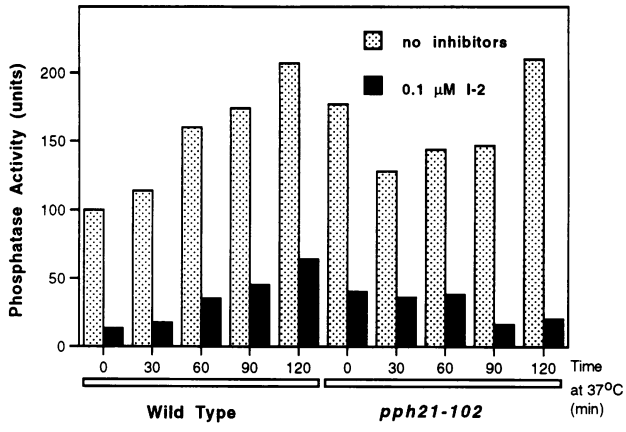

Fig. 8. Phosphatase activities in extracts from wild-type and *pph21-102* cells after shifting to the non-permissive temperature. A wild-type strain (CY2999) and a *pph21-102* mutant (CY3087) were arrested with hydroxyurea, released and then shifted to 37°C as described in the legend to Figure 5. Samples were taken at the indicated times. The extracts were preincubated for 10 min at 30°C either with (0.1 μM) or without inhibitor I-2. Phosphatase reactions were performed for 10 min at 30°C in the absence of divalent cations and at a protein concentration of 250 μg/ml. The phosphatase activity in the wild-type cells at the 0 time point was assigned to 100 U. The graphs are the average of two independent experiments.

pph21-102 cells compared with the wild-type cells (Figure 7C and F). Therefore, PP2A is required for the normal intrinsic activity of Clb2–Cdc28 kinase complexes.

PP2A activity in pph21-102 cells decreases after a shift to the non-permissive temperature

In *pph21-102* cells, the Clb2-associated kinase activity decreased after incubation at 37°C (Figure 6). To examine PP2A activity under the same conditions used in Figure 6, we prepared cell extracts from wild-type and *pph21-102* cells that were released from a hydroxyurea arrest and shifted to 37°C. The type 2A phosphatase activity was determined using phosphorylated histone H1 as the substrate, which was used previously to measure type 1 and 2A phosphatase activity in *S.cerevisiae* cell extracts (Sola *et al.*, 1991). The specific type 1 phosphatase inhibitor I-2 was used to inhibit type 1 phosphatase activity. The I-2 independent H1 phosphatase activity corresponds mostly to type 2A phosphatase activity. As shown in Figure 8, the H1 phosphatase activities in the absence of I-2 increased after a shift to the non-permissive temperature in both wild-type and *pph21-102* cells. However, in the presence of I-2 the H1 phosphatase activity for the wild-type cells increased ~3-fold during the 2 h incubation at 37°C, while the H1 phosphatase activity for the *pph21-102* cells decreased to ~50% of starting levels. These results suggest that the type 2A phosphatase activity in *pph21-102* cells was defective after a shift to the non-permissive temperature.

It should be noted that at the 0 h time point (24°C) the H1 phosphatase activity was higher in the hydroxyurea-arrested *pph21-102* cells than in the wild-type cells, in both the absence and presence of I-2 (Figure 8). The same relative increases in phosphatase activities was also seen for extracts prepared from asynchronous *pph21-102* and wild-type cells grown at 24°C (data not shown). Possibly, the Pph21-102 protein may have a lower association with negative regulatory subunits.

PP2A-deficient cells are sensitive to the loss of MIH1

As shown above, a defect in PP2A function causes a delay or block in G2 and a loss of Clb2–Cdc28 kinase activity, arguing that PP2A is a positive factor for entry into mitosis in budding yeast. These findings differ from the role of PP2A described in *S.pombe* and *Xenopus* (see Introduction). To confirm that *S.cerevisiae* PP2A is required for the advancement from G2 into M phase, a genetic analysis between PP2A genes *SWE1* and *MIH1* was performed. *SWE1* and *MIH1* are *S.cerevisiae* homologs of *wee1*$^+$ and *cdc25*$^+$, respectively. The deletion of either *SWE1* and *MIH1* alone had no effect on the growth rate of the cells (Russell *et al.*, 1989; Booher *et al.*, 1993). We crossed a Δ*pph21* Δ*pph22* mutant with either a Δ*swe1* mutant or a Δ*mih1* mutant. The growth rate of the Δ*pph21* Δ*pph22* Δ*swe1* mutants was very similar to that of the Δ*pph21* Δ*pph22* mutants (data not shown). However, the Δ*pph21* Δ*pph22* Δ*mih1* mutants had a much more severe growth defect than the Δ*pph21* Δ*pph22* mutants (Figure 9A), and most of the Δ*pph21* Δ*pph22* Δ*mih1* cells had elongated buds (Figure 9B, plates a and b). This elongated bud phenotype is similar to that seen in a Δ*mih1* strain in which *wee1*$^+$ or *SWE1* is overexpressed, which causes a long mitotic delay (Russell *et al.*, 1989; Booher *et al.*, 1993). Therefore, unlike wild-type cells, Δ*pph21* Δ*pph22* cells are sensitive to the loss of *MIH1*, suggesting that both PP2A and Mih1 function as positive factors for the progression from G2 into mitosis.

Deletion of *MIH1* causes an accumulation of 2N DNA cells, probably due to a mitotic delay (Russell *et al.*, 1989; Booher *et al.*, 1993). This accumulation of 2N DNA cells in Δ*mih1* cultures was eliminated by the *cdc28F19* mutation, where a phenylalanine was substituted for tyrosine 19 (data not shown). This finding agrees with the notion that Mih1 is a tyrosine phosphatase that is able to activate the Cdc28 kinase via tyrosine 19 dephosphorylation. Therefore, we expected that the more severe growth defect of a Δ*pph21* Δ*pph22* Δ*mih1* mutant should be rescued by the *cdc28F19* mutation. Not only was the severe growth defect of the Δ*pph21* Δ*pph22* Δ*mih1* mutant eliminated by the *cdc28F19* mutation (Figure 9A), but the elongated bud phenotype was also suppressed (Figure 9B). Therefore, the synthetic growth and morphology defects due to the loss of *MIH1* in PP2A-deficient cells are specific to the function of *CDC28*.

The effect of the cdc28F19 mutation on Clb2–Cdc28 kinase activity

Both PP2A and Mih1 may have positive roles in mitotic entry and in activation of the Cdc28 kinase. We asked whether the *cdc28F19* mutation has any effect on Cdc28 kinase activity in wild-type and *pph21-102* cells before and after mitotic initiation. We compared four strains: wild-type, *pph21-102*, *cdc28F19* and *pph21-102 cdc28F19*. These four strains were arrested in either S phase by hydroxyurea or M phase by nocodazole at the permissive temperature (24°C) and examined for their Clb2-associated kinase activity. At the hydroxyurea arrest, the *cdc28F19* cells and the *pph21-102 cdc28F19* cells had a high kinase activity, almost twice as much as for the wild-type cells and at least three times as high as for *pph21-102* cells (Figure 5D). Similar results were obtained

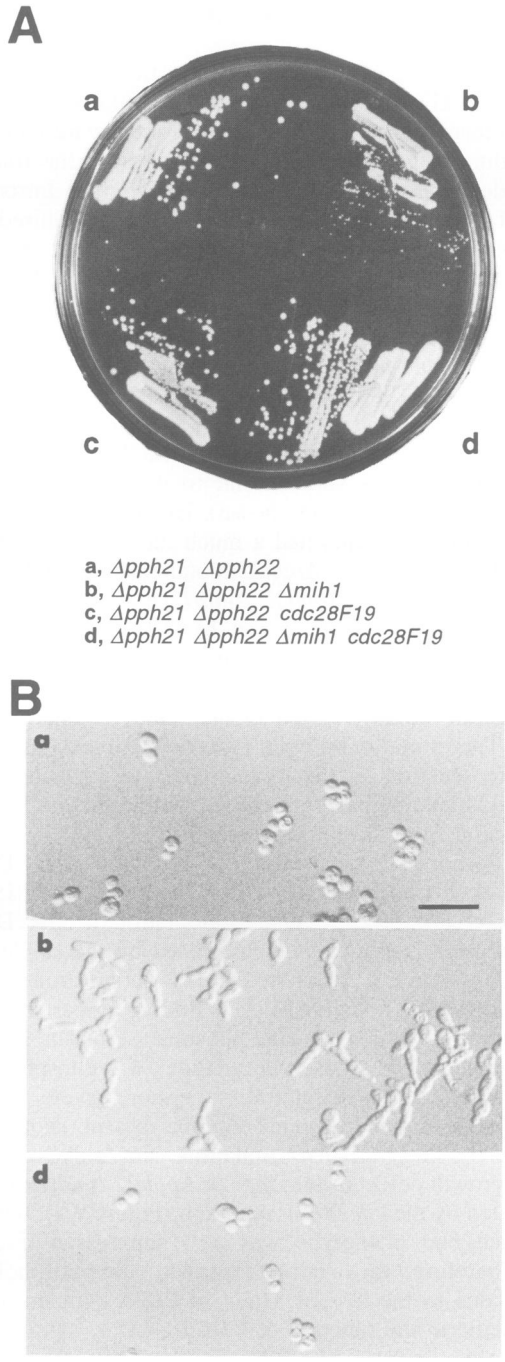

Fig. 9. PP2A mutants are sensitive to the loss of *MIH1*. (**A**) Strains (a) *Δpph21 Δpph22* (CY1145), (b) *Δpph21 Δpph22 Δmih1* (CY3831), (c) *Δpph21 Δpph22 cdc28F19* (CY3832) and (d) *Δpph21 Δpph22 Δmih1 cdc28F19* (CY3833) were streaked onto a YEPD plate and incubated at 24°C for 4 days. Strain CY3831 was a representative segregant derived from a cross between a *Δpph22 Δpph21* mutant (CY1145) and a *Δmih1* mutant (CY3074; 32 tetrads were dissected). Strains CY3832 and CY3833 were representative segregants obtained from a cross between CY3831 and CY2847 (40 tetrads were dissected). (**B**) Photographs of (a) *Δpph21 Δpph22* (CY1145), (b) *Δpph21 Δpph22 Δmih1* (CY3831) and (d) *Δpph21 Δpph22 Δmih1 cdc28F19* (CY3833) cells, which were grown to log phase in YEPD medium. Bar, 17 μm.

using p^{13}-Sepharose beads (Brizuela *et al.*, 1987), which presumably bind all Clb–Cdc28 kinase complexes (data not shown). Our results are different from the previous report that the *cdc28F19* mutation does not increase Cdc28 kinase activity in hydroxyurea-arrested cells (Sorger and Murray, 1992). For the cells arrested in M phase by nocodazole at 24°C, the Clb2-associated kinase activity in all four strains was high and showed little difference from each other (Figure 5D). Based on these results, we suggest that the *cdc28F19* mutation is able to partially activate the Clb2–Cdc28 kinase prior to mitosis.

Because the *pph21-102 cdc28F19* cells had high kinase activity at the hydroxyurea arrest at the permissive temperature, we determined if such a high kinase activity is maintained and if it can override the defect due to the *pph21-102* mutation at the non-permissive temperature. Upon release from the hydroxyurea arrest, the total amount of Clb2-associated kinase activity for the *pph21-102 cdc28F19* cells decreased with similar kinetics as for the *pph21-102* cells during incubation at 37°C (Figure 6A and D). Therefore, a mutation preventing tyrosine 19 phosphorylation in Cdc28 kinase did not bypass the requirement for PP2A to maintain high total levels of Clb2-associated kinase activity. However, the *pph21-102 cdc28F19* cells did have a higher specific activity of Clb2-associated kinase than the *pph21-102* cells after 2 h incubation at 37°C (Figure 6C). Moreover, 7 (0 h), 22 (after 2 h) and 16% (after 4 h) of the *pph21-102 cdc28F19* cells were unbudded after a release from the hydroxyurea arrest and a shift to 37°C (Figure 5A and C). Therefore, *pph21-102* cells expressing Clb2 from the *S.cerevisiae ADH* promoter or with a *cdc28F19* mutation had increased total amounts of Clb2–Cdc28 kinase activity (compared with *pph21-102* cells expressing Clb2 only from the native promoter), which resulted in more cells passing through the first mitosis. However, these higher levels of total Clb2–Cdc28 kinase activity were not able to fully suppress the G2 block of the *pph21-102* cells, suggesting either that the low specific activity of the Clb2–Cdc28 complexes in the *pph21-102* cells causes the block (see Figure 6 and Figure 7), or that PP2A is required for an additional process in G2.

Discussion

PP2A, actin cytoskeleton and bud morphogenesis

Both *cdc55* cells and *tpd3* cells have abnormally elongated buds and a delay or partial block in cytokinesis (Healy *et al.*, 1991; van Zyl *et al.*, 1992). Tpd3 and Cdc55 are *S.cerevisiae* homologs of mammalian A and B regulatory subunits of PP2A, respectively. Ronne *et al.* (1991) observed that PP2A-depleted cells have heterogeneous morphological defects in the growing bud. When grown at the non-permissive temperature, *pph21-102* cells arrest primarily with small or abnormally shaped buds (Figure 2B). Therefore, our data confirm the role of PP2A in bud growth and morphogenesis.

In *S.cerevisiae*, the shape of the bud is determined by the temporal coordination of apical and spherical growth. Apical growth predominates during the early budded stage, but spherical growth prevails after the medium-sized bud stage (Farkas *et al.*, 1974). That various stages of bud growth have a particular actin distribution during the cell cycle, along with the phenotypes of cytoskeleton mutants (Welch *et al.*, 1994), led to a hypothesis that the actin cytoskeleton functions to direct cell surface growth. In

this model, apical growth is due to a polarized actin distribution, whereas spherical growth results from a more uniform distribution of actin. Our results show that a lack of normal PP2A function perturbs the distribution of actin patches and cables. These defects in actin organization might be responsible for both the aberrant bud morphology and the abnormal chitin deposition in the arrested *pph21-102* cells. Three possible functional pathways are proposed. First, PP2A may function directly on the actin cytoskeleton during the cell cycle, and subsequently might direct the mode of cell surface growth to determine bud shape. Second, PP2A might regulate the bud site complex, which is responsible for bud emergence and growth, possibly through a regulation of the actin distribution (Chant and Pringle, 1991; Welch *et al.*, 1994). We observed that a deletion of *BEM2*, which encodes a component of the bud site complex (Chant and Pringle, 1991), is lethal in a *Δpph21 Δpph22* mutant (data not shown). Third, the effect of PP2A on actin distribution may be via the effect of PP2A on Clb–Cdc28 kinase activity (this paper). An active Clb–Cdc28 kinase was reported to be necessary for switching to spherical growth of the bud by a depolarization of the cortical actin patches (Lew and Reed, 1993).

Budding yeast PP2A plays a positive role in progression from G2 into mitosis

Three lines of evidence suggest that PP2A plays a positive role for entry into mitosis in *S.cerevisiae*. First, at the non-permissive temperature *pph21-102* cells arrest in a G2-like stage, with a bud, a 2N DNA content, an undivided nucleus and either a single microtubule organizing center (74% of cells) or a short mitotic spindle (11% of cells). Second, an extended G2 phase was seen in *Δpph22 Δpph21* cells which have very little PP2A activity provided by Pph3. Third, unlike wild-type cells, *Δpph22 Δpph21* cells are sensitive to the loss of *MIH1*. These findings raise the possibility that in *S.cerevisiae*, PP2A may be involved in a pathway that positively regulates progression from G2 into M phase.

This positive role of *S.cerevisiae* PP2A in mitotic initiation is opposite to the proposed role of PP2A in *S.pombe* and *Xenopus*, where PP2A seems to negatively regulate entry into mitosis (see Introduction). There are three possible explanations for these differences. First, PP2A may function differently in the initiation of mitosis in the different organisms. Second, the *pph21-102* mutation may result in hyperactivation of PP2A instead of loss of PP2A activity. However, the *Δpph22 Δpph21* mutants have a G2 delay, compared with G2 block in the arrested *pph21-102* cells. Moreover, results from the protein phosphatase assays (Figure 8) suggest that *pph21-102* cells have reduced PP2A activity at the restrictive temperature. Therefore, G2 block of the arrested *pph21-102* cells is probably not due to a hyperactive PP2A. Third, two different forms of PP2A may coexist in the same organism. One would play a negative role to prevent mitosis during late S or early G2 phase and the other would act at the G2/M phase to trigger mitosis. The *pph21-102* alteration would inactivate the latter form of PP2A. The identification or purification of such a unique form of PP2A in *S.cerevisiae* may resolve this question.

PP2A is involved in a crucial pathway required for activation of the Clb–Cdc28 kinase complex

The cdc25–wee1 pathway is critical for the regulation of the cdc2 kinase at G2/M in *Xenopus* and *S.pombe* (see Introduction). The corresponding Mih1–Swe1 pathway in budding yeast appears not to be critical for entry into mitosis. Unlike cdc2 in *S.pombe*, mutation of the equivalent tyrosine to phenylalanine in Cdc28 is not able to accelerate significantly the onset of mitosis in *S.cerevisiae* (Amon *et al.*, 1992; Sorger and Murray, 1992). Russell *et al.* (1989) and Booher *et al.* (1993) have reported that overexpression of the *S.pombe* wee1 kinase or *S.cerevisiae* Swe1 kinase in *Δmih1* mutants can prevent cells from undergoing mitosis. We have observed that the mitotic delay caused by a deletion of *MIH1* (Russell *et al.*, 1989) can be eliminated by the *cdc28F19* mutation (data not shown). Although the deletion of *MIH1* has no effect on the growth rate of wild-type cells, PP2A-deficient cells are sensitive to the loss of *MIH1*. This sensitivity can be rescued by the *cdc28F19* mutation. Therefore, the regulation of Cdc28 kinase activity by the Mih1–Swe1 pathway becomes critical when PP2A activity is low. At the hydroxyurea arrest, the *cdc28F19* mutation resulted in a ≥2-fold more specific activity of Clb2–Cdc28 kinase in wild-type or *pph21-102* cells at the permissive temperature (see time point 0 in Figure 6C), and allows some of the *pph21-102* cells to pass through mitosis in the first cell cycle (Figure 5A and C). However, the *cdc28F19* mutation is not able to prevent the decrease in Clb2–Cdc28 kinase activity (total or specific) in the *pph21-102* cells shifted to the non-permissive temperature (Figure 6A and C). Therefore, the budding yeast Mih1–Swe1 pathway may play a minor role in regulating Clb–Cdc28 kinase activity for the onset of mitosis. It is possible that PP2A may be required for a major pathway that activates the Clb–Cdc28 kinase for progression from G2 into mitosis.

We have shown that PP2A is required for normal Clb2–Cdc28 kinase activity (Figure 6). A moderate reduction in *CLB2* RNA levels was also observed when the *pph21-102* cells were shifted to the non-permissive temperature, probably because *CLB2* transcription requires Clb2–Cdc28 kinase activity (data not shown). Expression of Clb2 from the heterologous promoters increased the levels of Clb2 and its total levels of associated kinase activity in the *pph21-102* cells (compared with cells expressing Clb2 from the native promoter). However, for Clb2 expressed from the heterologous promoters, the specific kinase activity of the Clb2–Cdc28 complexes was lower in the *pph21-102* cells at the non-permissive temperature compared with wild-type cells (Figure 7). These results suggest that the effect of PP2A on Clb2–Cdc28 kinase activity is probably via a post-translational effect. Phosphorylation of cdc2 at threonine 161 in *Xenopus* or 167 in *S.pombe* is required for cdc2 kinase activity (Ducommun *et al.*, 1991; Gould *et al.*, 1991; Solomon *et al.*, 1992). A kinase that phosphorylates cdc2, CAK, has been purified from *Xenopus* extracts and identified in human cells (Solomon *et al.*, 1992; Fisher and Morgan, 1994; Makela *et al.*, 1994). One possibility is that PP2A is required to activate a *S.cerevisiae* CAK homolog, which would directly activate the Clb–Cdc28 kinase. As an alternative to PP2A regulating the post-translational modifications of

Table I. Strain list

Strain	Genotype	Source
W303	*MATa ura3-1 leu2-3,112 his3-11,15 trp1-1 ade2-1 can1-100*	R.Rothstein
CY403	*MATα pph22::HIS3 W303*	Sutton *et al.* (1991a)
CY1080	*MATα pph3::LEU2 W303*	Ronne *et al.* (1991)
CY1145	*MATa pph22::HIS3 pph21::URA3 W303*	this work
CY1435	*MATa pph22::HIS3 pph21::HIS3 W303*	this work
CY1619	*MATa pph22::HIS3 pph21::HIS3 pph3::LEU2 [PPH21/YCp50] W303*	this work
CY1678	*MATa pph22::HIS3 pph21::HIS3 pph3::LEU2 [PPH21/TRP1/CEN] W303*	this work
CY2696	*MATα bem2::LEU2 ura3-1 leu2-3,112 his3-11,15*	this work
CY2848	*MATα cdc28F19 W303*	P.Sorger
CY2999	*MATa CLB2-HA W303*	this work
CY3006	*MATa pph22::HIS3 pph21::HIS3 pph3::LEU2 [pph21-102/TRP1/CEN] W303*	this work
CY3007	*MATa pph22::HIS3 pph21::HIS3 pph3::LEU2 [pph21-102/YCp50] W303*	this work
CY3008	*MATa pph22::HIS3 pph21::HIS3 pph3::LEU2 cdc28F19 [pph21-102/YCp50] W303*	this work
CY3010	*MATα pph22::HIS3 pph21::HIS3 pph3::LEU2 cdc28F19 [pph21-102/YCp50] W303*	this work
CY3016	*MATa CLB2-HA pph22::HIS3 pph21::HIS3 pph3::LEU2 [pph21-102/TRP1/CEN] W303*	this work
CY3074	*MATa mih1::LEU2 ura3-1 leu2-3,112 his3-11,15 trp1-1*	P.Sorger
CY3087	*MATa CLB2-HA pph22::HIS3 pph21::HIS3 pph3::LEU2 [pph21-102/YCp50] W303*	this work
CY3089	*MATa CLB2-HA pph22::HIS3 pph21::HIS3 pph3::LEU2 cdc28F19 [pph21-102/YCp50] W303*	this work
CY3256	*MATa CLB2-HA cdc28F19 W303*	this work
CY3831	*MATa pph22::HIS3 pph21::URA3 mih1::LEU2 ura3-1 leu2-3,112 his3-11,15 trp1-1*	this work
CY3832	*MATa pph22::HIS3 pph21::URA3 cdc28F19::TRP1 ura3-1 leu2-3,112 his3-11,15 trp1-1*	this work
CY3833	*MATa pph22::HIS3 pph21::URA3 mih1::LEU2 cdc28F19 ura3-1 leu2-3,112 his3-11,15 trp1-1*	this work
CY3866	*MATα swe1::LEU2 ura3-1 leu2-3,112 his3-11,15 trp1-1*	this work
CY4279	*MATa [S.pombe ADH:CLB2-HA/YCp50] W303*	this work
CY4280	*MATa pph22::HIS3 pph21::HIS3 pph3::LEU2 [pph21-102/TRP1/CEN] [S.pombe ADH:CLB2-HA/YCp50] W303*	this work
CY4281	*MATa CLB2-HA pph22::HIS3 pph21::HIS3 pph3::LEU2 [pph21-102/TRP1/CEN] [S.pombe ADH/YCp50] W303*	this work
CY4294	*MATa ura3-1 leu2-3,112 his3-11,15 trp1-1 ade2-1 can1-100 [S.cerevisiae ADH:CLB2-HA/YCp50] W303*	this work
CY4296	*MATa pph22::HIS3 pph21::HIS3 pph3::LEU2 [pph21-102/TRP1/CEN] [S.cerevisiae ADH:CLB2-HA/YCp50] W303*	this work
CY4299	*MATa CLB2-HA pph22::HIS3 pph21::HIS3 pph3::LEU2 [pph21-102/TRP1/CEN] [S.cerevisiae ADH/YCp50] W303*	this work

the Clb–Cdc28 kinase, loss of PP2A activity may result in increased levels, activity or association of an inhibitor of the Clb–Cdc28 kinase, such as p40 (Mendenhall, 1993; Nugroho and Mendenhall, 1994). The testing of these hypotheses may uncover *S.cerevisiae* PP2A regulatory pathways that control the activity of Clb–Cdc28 kinase complexes.

Materials and methods

Strains and media

Yeast strains used in this study are listed in Table I. *S.cerevisiae* mutations *pph3::LEU2* (Ronne *et al.*, 1991), *mih1::LEU2* (Russell *et al.*, 1989), *swe1::LEU2* (Booher *et al.*, 1993) and *cdc28F19* (Sorger and Murray, 1992) have been described previously. The *bem2* (also called *ipl2*) *::LEU2* mutant was provided by Clarence Chan. Cells were grown in YEPD medium (1% yeast extract, 2% Bacto-peptone and 2% glucose).

Isolation of the PPH21 gene

A 1.3 kb *Bst*BI fragment of *PPH22*, containing the entire open reading frame (ORF), was used to screen a *S.cerevisiae* genomic DNA library in YCp50 (Rose *et al.*, 1987). Plasmid DNA was isolated from 18 positive clones and restriction enzyme digestion revealed one class of novel gene. By Southern blot analysis, the *PPH22*-hybridizing region was localized to a 2.1 kb *Xba*I–*Xho*I fragment. The fragment was subcloned and sequenced on both strands (Sanger *et al.*, 1977). The complete coding region was found to be contained within the 2.1 kb *Xba*I–*Xho*I fragment, which was cloned into the blunted *Xba*I site of pUC118, yielding plasmid pCB1048. The DNA sequence and predicted amino acid sequence of this gene are highly similar to that of *PPH22* (*PPH2α* in Sutton *et al.*, 1991a). This gene is the same as *PPH21* reported by Sneddon *et al.* (1990) and Ronne *et al.* (1991).

Preparation of PPH21 deletion alleles

The null alleles *pph21::URA3* and *pph21::HIS3* were constructed as follows. A 1.2 kb *Hin*dIII fragment containing the *URA3* gene, or a 1.8 kb *Bam*HI fragment containing the *HIS3* gene, was inserted in place of the *Eco*RI–*Bgl*II fragment within *PPH21* in pCB1048. The *pph21* deletion allele was then excised using *Sal*I and *Bam*HI, and was used to transform strain W303 to replace the wild-type *PPH21* gene. The chromosomal deletion was confirmed by Southern blot analysis. The *pph21* deletion mutants were mated with CY403. The diploids were sporulated and the tetrads were dissected to obtain haploid *Δpph22 Δpph21* mutants, CY1145 and CY1435.

Preparation of a temperature-sensitive PPH21 allele

A 3.2 kb *Bst*EII–*Spe*I fragment encompassing the entire *PPH21* ORF was subcloned into the *Pst*I–*Xba*I sites of pUC118, yielding plasmid pCB1348. Oligonucleotide-directed mutagenesis (Kunkel, 1985) was performed to generate the *pph21-102* mutation using the oligonucleotide 5′-ACGTGTTGCAGTTC**A**AGGAGAATGTTAAA-3′. The substituted base is in bold. The *pph21-102* mutation was confirmed by DNA sequence analysis. A 3.2 kb *Sph*I–*Bam*HI fragment, containing either the PPH21 gene or the *pph21-102* gene, was subcloned into the *Sph*I–*Bam*HI site of a *TRP1/CEN* plasmid. The resulting plasmids were transformed into a strain lacking *PPH22*, *PPH21* and *PPH3* but kept alive by a YCp50 plasmid carrying *PPH21* (CY1619). The transformants were selected for 5-fluoro-orotic acid resistance (Boeke *et al.*, 1984) to obtain a *pph21-102* strain (CY3006) without *PPH21*/YCp50. A *pph21-102/YCp50* plasmid was introduced into CY3006, and then the *pph21-102/TRP/CEN* plasmid was lost. The resulting strain, CY3007, was mated with CY2848, which contains the *cdc28F19* mutation and was provided by Peter Sorger. The diploid was sporulated to obtain a haploid *pph21-102 cdc28F19* segregant, CY3008.

Epitope-tagged Clb2 strains

A 2.8 kb *Xho*I–*Eco*RI fragment of *CLB2* from plasmid pIC19 (Fitch *et al.*, 1992) was cloned into vector pUC118 to produce plasmid pCB1581. By oligonucleotide-directed mutagenesis (Kunkel, 1985), a unique *Not*I site was created just upstream of the *CLB2* stop codon using the oligonucleotide 5′-CATCTGCCCCTCTTCTCA**GCGGCC-GC**CTTCATGCAAGGTCATTAT-3′. The *Not*I restriction site is in bold. A 110 bp DNA fragment decoding a triple tandem HA1 epitope (Field *et al.*, 1988; Tyers *et al.*, 1992) was inserted into the *Not*I site, resulting in plasmid pCB1593. Alleles containing this epitope tag are designated *CLB2-HA*, which fully complemented for the *CLB2* gene. The *CLB2-HA* allele was used to replace the *CLB2* gene in either W303 or CY3006, yielding CY2999 (*CLB2-HA*) and CY3016 (*pph21-102/TRP1/*

CEN CLB2-HA). Strain CY3016 was mated to CY3010 to generate haploid strains CY3087 and CY3089. CY3256 was derived from a cross between CY2999 and CY2848. To construct *CLB2-HA* transcribed from heterologous promoters, we used oligonucleotide-directed mutagenesis (Kunkel, 1985) to create a second *Cla*I site on plasmid pCB1581 immediately upstream of the *CLB2* start codon with the oligonucleotide 5′-TTGGACATCTATAAG**ATCGAT**GAAGAGAGAGAGGGG-3′. Then, a 0.7 kb *Hin*dIII fragment of pCB1593, containing HA1 epitope coding sequences at the C-terminus of Clb2, was used to replace the equivalent fragment in pCB1581, resulting in a plasmid carrying *CLB2-HA* which had two *Cla*I sites. The 1.6 kb *Cla*I fragment of *CLB2-HA* was placed downstream of the *S.pombe ADH* promoter or *S.cerevisiae ADH* promoter, yielding *S.pombe ADH:CLB2-HA/YCp50* and *S.cerevisiae ADH:CLB2-HA/YCp50*. These two plasmids were transformed into either W303 or CY3006 to generate CY4279, CY4280, CY4294 and CY4296 strains. Strains containing *CLB2-HA*, CY2999, CY3256, CY3087, CY3089, CY4279, CY4280, CY4294 and CY4296 were shown to produce Clb2-HA protein by Western blot analysis using anti-HA monoclonal antibodies 12CA5.

Size analysis, flow cytometry, cell counting and microscopy

Cell size was determined with a Coulter Channelyzer as described previously (Tyers *et al.*, 1993). Flow cytometry was performed as described previously (Fernandez-Sarabia *et al.*, 1992) using either an EFP or an EPICS Coulter Elite flow cytometer. Yeast cells were fixed overnight in 70% ethanol at 4°C, washed and resuspended in PBS buffer. Cell density and budding index were determined using a hemacytometer.

Cells were processed for fluorescence and indirect immunofluorescence microscopy as described (Rose and Fink, 1987). DNA was visualized by DAPI staining at 1 μg/ml. Tubulin was visualized using YOL/34 (Serb Laboratory) as the primary antibody at a 1:200 dilution, and G-fluorescein isothiocyanate-conjugated goat anti-rat antibody (Boehringer Mannheim) as secondary antibodies at a 1:50 dilution. Fixation of cells and the subsequent rhodamine phalloidin (Molecular Probes) or Calcoflour (Fluorescent Brightner 28; Sigma) staining were performed as described previously (Pringle, 1991; Pringle *et al.*, 1991). All photographs were taken with a Nikon Optiphot microscope on Kodak Tmax-3200 film at 3200 ASA.

Cell cycle synchronization

Cultures were grown exponentially at 24°C in YEPD medium, diluted to an OD_{600} of 0.2, and hydroxyurea (Fluka) was added at a final concentration of 0.2 M. After 3 h at 24°C, the S phase arrested cells were filtered, washed with YEPD medium, resuspended in fresh medium and shifted to 37°C. Cultures were synchronized in M phase by adding nocodazole (Sigma) at a final concentration of 15 μg/ml to exponentially growing cells at an OD_{600} of 0.2, and incubating at 24°C for 3 h.

Cell extracts, immunoprecipitations, immunoblotting and kinase assays

Approximately 1×10^8 cells of the indicated strain were harvested by centrifugation at 4°C, washed with ice-cold buffer TENN (50 mM Tris, pH 7.5, 10 mM EDTA, 250 mM NaCl, 0.1% NP-40) and resuspended in 200 μl of TENN buffer containing protease and phosphatase inhibitors (1 mM phenylmethylsulfonyl fluoride, 1 μg/ml leupeptin, 1 μg/ml pepstatin, 0.6 mM dimethylaminopurine, 10 μg/ml soybean trypsin inhibitor, 1 μg/ml *N*-tosyl-L-phenylalanine chloromethyl ketone, 1 mM sodium orthovanadate, 10 mM sodium fluoride and 1 mM sodium pyrophosphate). Soluble cell extracts were prepared and Clb2-HA was immunoprecipitated from the extracts (0.5 mg total protein) using 1.0 μl of 12CA5 ascites fluid as described previously (Tyers *et al.*, 1992). For Western blot analysis, the Clb2-HA immunoprecipitates were resuspended in 2× loading buffer, heated at 95°C for 5 min and loaded onto an 8% SDS–polyacrylamide gel (Laemmli, 1970). The gel was electroblotted onto Immobilon membrane (Millipore). Clb2-HA was detected with a 1:5000 dilution of 12CA5 ascites fluid, and the Cdc28 was detected with a 1:2000 dilution of anti-Cdc28 antiserum (a gift from Kim Nasmyth), both using ECL methods (Amersham). A Laser Densitometer 110A (Molecular Dynamics) was used to quantitate Clb2 and Cdc28 levels.

For kinase assays, half the amount of Clb2-HA immunoprecipitates used for the Western blot was used and preincubated at 37°C for 5 min. Subsequently, 8 μl of 50 mM Tris–HCl, pH 7.4, 10 mM $MgCl_2$, 750 μM ATP, 2 μg bovine histone H1 (Boehringer Mannheim) and 10 μCi 5′-[γ-^{32}P]ATP (Amersham) were added. The reaction was incubated at 37°C for 10 min and was stopped by adding 30 μl of 2× loading buffer, then heating at 95°C for 5 min prior to loading on an 8% SDS–polyacrylamide gel. After the gel was fixed and dried, the phosphorylated H1 was visualized by autoradiography. The quantitative measurement of ^{32}P incorporation for each sample was performed with a Fuji Phosphorimager BAS-2000.

Protein phosphatase assays

Cell extracts were prepared as described previously (Cohen *et al.*, 1989). ^{32}P-labeled calf thymus histone H1 (Boehringer Mannheim) was prepared by phosphorylation with cyclic AMP-dependent protein kinase (UBI) in the reaction buffer 20 mM Tris–HCl, pH 7.5, 1 mM EGTA, 10 mM $MgCl_2$, 0.1% 2-mercaptoethanol, 0.1 mM ATP and [γ-^{32}P]ATP (~10^6 c.p.m./nmol). The reaction mixture was applied to a Microspin Column S-300HR (Pharmacia), using the procedures in the manufacturer's instructions to collect the labeled histone H1 in 20 mM Tris–HCl, pH 7.5, which was then extensively dialyzed. The assays of protein phosphatase activity followed the procedures of Cohen *et al.* (1988). The bacterially expressed human inhibitor 2 (a gift from N.Helps and P.T.W.Cohen) was used in the assays to inhibit the activity of type 1 phosphatase (Helps *et al.*, 1994). The reactions were terminated by the addition of 270 μl of charcoal solution (0.9 M HCl, 90 mM $Na_4P_2O_7$, 2 mM NaH_2PO_4 and 10% NoriA charcoal). The mixtures were centrifuged and the supernatant counted to measure the release of ^{32}P inorganic phosphate, as described by Flint *et al.* (1993).

Acknowledgements

We thank Clarence Chan, Robert Booher, James Broach, Marc Kirschner, John Pringle, Hans Ronne, Paul Russell and Peter Sorger for yeast strains and plasmids, Nicholas Helps and Patricia T.W.Cohen for human protein phosphatase inhibitor 2, Kim Nasmyth for the anti-Cdc28 polyclonal antibodies and Gerald Latter for advice on using the QUEST Protein Database Center funded by NCRR P41-RR02188. Helpful comments on the manuscripts were made by Ann Sutton and Bruce Futcher. F.C.L. was supported by a NIH postdoctoral fellowship. This research was funded by NIH grant no. GM45179 to K.T.A.

References

Adams,A.E. and Pringle,J.R. (1984) Relationship of actin and tubulin distribution to bud growth in wild-type and morphogenetic-mutant *S. cerevisiae*. *J. Cell Biol.*, **98**, 934–945.

Amon,A., Surana,U., Muroff,I. and Nasmyth,K. (1992) Regulation of p34^{CDC28} tyrosine phosphorylation is not required for entry into mitosis in *S. cerevisiae*. *Nature*, **355**, 368–371.

Amon,A., Tyers,M., Futcher,B. and Nasmyth,K. (1993) Mechanisms that help the yeast cell cycle clock tick: G2 cyclins transcriptionally activate G2 cyclins and repress G1 cyclins. *Cell*, **74**, 993–1007.

Bender,A. and Pringle,J.R. (1991) Use of a screen for synthetic lethal and multicopy suppressor mutants to identify two new genes involved in morphogenesis in *S. cerevisiae*. *Mol. Cell. Biol.*, **11**, 1295–1305.

Boeke,J.D., Lacroute,F. and Fink,G.R. (1984) A positive selection for mutants lacking orotidine-5′-phosphate decarboxylase activity in yeast: 5-fluoro-orotic acid resistance. *Mol. Gen. Genet.*, **197**, 345–346.

Booher,R.N., Deshaies,R.J. and Kirschner,M.W. (1993) Properties of *S. cerevisiae* wee1 and its differential regulation of p34^{CDC28} in response to G1 and G2 cyclins. *EMBO J.*, **12**, 3417–3426.

Brizuela,L., Draetta,G. and Beach,D. (1987) p13^{suc1} acts in the fission yeast cell division cycle as a component of the p34^{cdc2} protein kinase. *EMBO J.*, **6**, 3507–3514.

Byers,B. (1981) Cytology of the yeast life cycle. In Strathern,J.F., Jones,E.W. and Broach,J.R. (eds), *The Molecular Biology of the Yeast Saccharomyces*. Cold Spring Harbor Laboratory Press, Cold Spring Harbor, NY, pp. 59–96.

Chant,J. and Pringle,J.R. (1991) Budding and cell polarity in *Saccharomyces cerevisiae*. *Curr. Opin. Genet. Dev.*, **1**, 342–350.

Cohen,P., Alemany,S., Hemmings,B.A., Resink,T.J., Stralfors,P. and Tung,H.Y.L. (1988) Protein phosphatase-1 and protein phosphatase-2A from rabbit skeletal muscle. *Methods Enzymol.*, **159**, 390–408.

Cohen,P., Schelling,D.L. and Stark,J.R. (1989) Remarkable similarities between yeast and mammalian protein phosphatases. *FEBS Lett.*, **250**, 601–606.

Drubin,D.G. (1991) Development of cell polarity in budding yeast. *Cell*, **65**, 1093–1096.

Drubin,D.G., Jones,H.D. and Wertman,K.F. (1993) Actin structure and function: roles in mitochondrial organization and morphogenesis in

budding yeast and identification of the phalloidin-binding site. *Mol. Cell. Biol.*, **4**, 1277–1294.

Ducommun,B., Brambilla,P., Felix,M.A., Franza,B.R., Karsenti,B. and Draetta,G. (1991) cdc2 phosphorylation is required for its interaction with cyclin. *EMBO J.*, **10**, 3311–3319.

Dunphy,W.G. and Kumagai,A. (1991) The cdc25 protein contains an intrinsic phosphatase activity. *Cell*, **67**, 189–196.

Dunphy,W.G. and Newport,J.W. (1989) Fission yeast p13 blocks mitotic activation and tyrosine dephosphorylation of the *Xenopus* cdc2 protein kinase. *Cell*, **58**, 181–191.

Farkas,V., Kovarik,J., Kosinova,A. and Bauer,S. (1974) Autoradiographic study of mannan incorporation into the growing walls of *S.cerevisiae*. *J. Bacteriol.*, **117**, 265–269.

Fernandez-Sarabia,M.J., Sutton,A., Zhong,T. and Arndt,K.T. (1992) SIT4 protein phosphatase is required for the normal accumulation of *SWI4*, *CLN1*, *CLN2* and *HCS26* RNAs during late G1. *Genes Dev.*, **6**, 2417–2428.

Field,J., Nikawa,J., Broek,D., MacDonald,B., Rodgers,L., Wilson,I.A., Lerner,R.A. and Wigler,M. (1988) Purification of a RAS-responsive adenylyl cyclase complex from *S.cerevisiae* by use of an epitope addition method. *Mol. Cell. Biol.*, **8**, 2159–2165.

Fisher,R.P. and Morgan,D.O. (1994) A novel cyclin associates with MO15/Cdk7 to form the CDK-activating kinase. *Cell*, **78**, 713–724.

Fitch,I., Dahmann,C., Surana,U., Amon,A., Nasmyth,K., Goetsch,L., Byers,B. and Futcher,B. (1992) Characterization of four B-type cyclin genes of the budding yeast *S.cerevisiae*. *Mol. Cell. Biol.*, **3**, 805–818.

Flint,A.J., Gebbink,F.G.B., Franza,B.R., Hill,D.E. and Tonks,N.K. (1993) Multi-site phosphorylation of the protein tyrosine phosphatase, PTP1B: identification of cell cycle regulated and phorbol ester stimulated sites of phosphorylation. *EMBO J.*, **12**, 1937–1946.

Gautier,J., Solomon,M.J., Booher,R.N., Bazan,J.F. and Kirschner,M.W. (1991) cdc25 is a specific tyrosine phosphatase that directly activates $p34^{cdc2}$. *Cell*, **67**, 197–211.

Ghiara,J.B., Richardson,H.E., Sugimoto,K., Henze,M., Lew,D.J., Wittenberg,C. and Reed,S.I. (1991) A cyclin B homolog in *S.cerevisiae*: chronic activation of the Cdc28 protein kinase by cyclin prevents exit from mitosis. *Cell*, **65**, 163–174.

Gould,K.L. and Nurse,P. (1989) Tyrosine phosphorylation of the fission yeast $cdc2^{+}$ protein kinase regulates entry into mitosis. *Nature*, **342**, 39–45.

Gould,K.L., Moreno,S., Owen,O.J., Sazer,S. and Nurse,P. (1991) Phosphorylation at Thr167 is required for *S.pombe* $p34^{cdc2}$ function. *EMBO J.*, **10**, 3297–3309.

Healy,A.M., Zolnierowicz,S., Stapleton,A.E., Goebl,M., DePaoli-Roach,A.A. and Pringle,J.R. (1991) *CDC55*, a *Saccharomyces cerevisiae* gene involved in cellular morphogenesis: identification, characterization, and homology to the B subunit of mammalian type 2A protein phosphatase. *Mol. Cell. Biol.*, **11**, 5767–5780.

Helps,N.R., Street,A.J., Elledge,S.J. and Cohen,P.T.W. (1994) Cloning of the complete coding region for human protein phosphatase inhibitor 2 using the two hybrid system and expression of inhibitor 2 in *E.coli*. *FEBS Lett.*, **340**, 93–98.

Kilmartin,J.V. and Adams,A.E. (1984) Structural rearrangements of tubulin and actin during the cell cycle of the yeast *Saccharomyces*. *J. Cell Biol.*, **98**, 922–933.

Kinoshita,N., Yamano,H., Niwa,H., Yoshida,Y. and Yanagida,M. (1993) Negative regulation of mitosis by the fission yeast protein phosphatase ppa2. *Genes Dev.*, **7**, 1059–1071.

Kumagai,A. and Dunphy,W.G. (1992) Regulation of the cdc25 protein during the cell cycle in *Xenopus* extracts. *Cell*, **70**, 139–151.

Kunkel,T.A. (1985) Rapid and efficient site specific mutagenesis without phenotypic selection. *Proc. Natl Acad. Sci. USA*, **82**, 488–492.

Laemmli,U.K. (1970) Cleavage of structure proteins during assembly of the head of bacteriophage T4. *Nature*, **227**, 680–685.

Lee,T.H., Solomon,M.J., Mumby,M.C. and Kirschner,M.W. (1991) INH, a negative regulator of MPF, is a form of protein phosphatase 2A. *Cell*, **64**, 415–423.

Lee,T.H., Turck,C. and Kirschner,M.W. (1994) Inhibition of cdc2 activation by INH/PP2A. *Mol. Cell. Biol.*, **5**, 323–338.

Lew,D.J. and Reed,S.I. (1993) Morphogenesis in the yeast cell cycle: regulation by Cdc28 and cyclins. *J. Cell Biol.*, **120**, 1305–1320.

Lundgren,K., Walworth,N., Booher,R., Dembski,M., Kirschner,M. and Beach,D. (1991) mik1 and wee1 cooperate in the inhibitory tyrosine phosphorylation of cdc2. *Cell*, **64**, 1111–1122.

Makela,T., Tassan,J.P., Nigg,E.A., Frutiger,S., Hughes,G.J. and Weinberg,R.A. (1994) A cyclin associated with the CDK-activating kinase MO15. *Nature*, **371**, 254–257.

Mendenhall,M.D. (1993) An inhibitor of $p34^{CDC28}$ protein kinase activity from *S.cerevisiae*. *Science*, **259**, 216–219.

Nugroho,T.T. and Mendenhall,M.D. (1994) An inhibitor of yeast cyclin-dependent protein kinase plays an important role in ensuring the genomic integrity of daughter cells. *Mol. Cell. Biol.*, **14**, 3320–3328.

Nurse,P. (1990) Universal control mechanism regulating onset of M-phase. *Nature*, **344**, 503–508.

Piggott,J.R., Rai,R., Carter,B.L., Reed,S.I. and Wittenberg,C. (1982) A bifunctional gene product involved in two phases of the yeast cell cycle mitotic role for the Cdc28 protein kinase of *S.cerevisiae*. *Nature*, **298**, 697–701.

Pringle,J.R. (1991) Staining of bud scars and other cell wall chitin with calcofluor. *Methods Enzymol.*, **194**, 732–735.

Pringle,J.R. and Hartwell,L.H. (1981) The *Saccharomyces cerevisiae* cell cycle. In Strathern,J.F., Jones,E.W. and Broach,J.R. (eds), *The Molecular Biology of the Yeast Saccharomyces*. Cold Spring Harbor Laboratory Press, Cold Spring Harbor, NY, pp. 97–142.

Pringle,J.R., Adams,A.E.M., Drubin,D.G. and Haarer,B.K. (1991) Immunofluorescence methods for yeast. *Methods Enzymol.*, **194**, 565–602.

Reed,S.I. and Wittenberg,C. (1990) Mitotic role for the Cdc28 protein kinase of *S.cerevisiae*. *Proc. Natl Acad. Sci. USA*, **87**, 5697–5701.

Richardson,H., Lew,D.L., Henze,M., Sugimoto,K. and Reed,S.I. (1992) Cyclin-B homologs in *S.cerevisiae* function in S phase and in G2. *Genes Dev.*, **6**, 2021–2034.

Ronne,H., Carlberg,M., Hu,G.Z. and Nehlin,J.O. (1991) Protein phosphatase 2A in *S.cerevisiae*: effects on cell growth and bud morphogenesis. *Mol. Cell. Biol.*, **11**, 4876–4884.

Rose,M.D. and Fink,G.R. (1987) KAR1, a gene required for function of both intranuclear and extranuclear microtubules in yeast. *Cell*, **48**, 1047–1060.

Rose,M.D., Novick,P., Thomas,J.H., Botstein,D. and Fink,G.R. (1987) A *S.cerevisiae* genomic plasmid bank based on a centromere-containing shuttle vector. *Gene*, **60**, 237–243.

Russell,P. and Nurse,P. (1987) Negative regulation of mitosis by $wee1^{+}$, a gene encoding a protein kinase homolog. *Cell*, **49**, 559–567.

Russell,P., Moreno,S. and Reed,S.I. (1989) Conservation of mitotic controls in fission and budding yeasts. *Cell*, **57**, 295–303.

Sanger,J.M., Nicklen,S. and Coulson,A. (1977) DNA sequencing with chain-terminating inhibitors. *Proc. Natl Acad. Sci. USA*, **86**, 8333–8337.

Sneddon,A.A., Cohen,P.T.W. and Stark,M. (1990) *S.cerevisiae* protein phosphatase 2A performs an essential cellular function and is encoded by two genes. *EMBO J.*, **9**, 4339–4346.

Sola,M.M., Langan,T. and Cohen,P. (1991) $p34^{cdc2}$ phosphorylation sites in histone H1 as dephosphorylated by protein phosphatase 2A1. *Biochim. Biophys. Acta*, **1094**, 211–216.

Solomon,M.J. (1993) Activation of the various cyclin/cdc2 protein kinases. *Curr. Opin. Cell Biol.*, **5**, 180–186.

Solomon,M.J., Glotzer,M., Lee,T.H., Philippe,M. and Kirschner,M.W. (1990) Cyclin activation of $p34^{cdc2}$. *Cell*, **63**, 1013–1024.

Solomon,M.J., Lee,T.H. and Kirschner,M.W. (1992) Role of phosphorylation in $p34^{cdc2}$ activation: identification of an activating kinase. *Mol. Cell. Biol.*, **3**, 13–27.

Sorger,P.K. and Murray,A.W. (1992) S-phase feedback control in budding yeast independent of tyrosine phosphorylation of $p34^{cdc28}$. *Nature*, **355**, 365–368.

Strausfeld,U., Labbe,J.C., Fesquet,D., Cavadore,J.C., Picard,A., Sadhu,K., Russell,P. and Doree,M. (1991) Dephosphorylation and activation of a $p34^{cdc2}$/cyclin B complex *in vitro* by human CDC25 protein. *Nature*, **351**, 242–245.

Surana,U., Robitsch,H., Price,C., Schuster,T., Fitch,I., Futcher,A.B. and Nasmyth,K. (1991) The role of CDC28 and cyclins during mitosis in the budding yeast *S.cerevisiae*. *Cell*, **65**, 145–161.

Sutton,A., Immanuel,D. and Arndt,K.T. (1991a) The SIT4 protein phosphatase functions in late G1 for progression into S phase. *Mol. Cell. Biol.*, **11**, 2133–2148.

Sutton,A., Lin,F., Fernandez-Sarabia,M.J. and Arndt,K.T. (1991b) The SIT4 protein phosphatase is required in late G1 for progression into S phase. *Cold Spring Harbor Symp. Quant. Biol.*, **56**, 21–31.

Tyers,M., Tokiwa,G., Nash,R. and Futcher,B. (1992) The Cln3–Cdc28 kinase complex of *S.cerevisiae* is regulated by proteolysis and phosphorylation. *EMBO J.*, **11**, 1773–1784.

Tyers,M., Tokiwa,G. and Futcher,B. (1993) Comparison of the *Saccharomyces cerevisiae* G1 cyclins: Cln3 may be an upstream activator of Cln1, Cln2 and other cyclins. *EMBO J.*, **12**, 1955–1968.

van Zyl,W., Huang,W., Sneddon,A.A., Stark,M., Camier,S., Werner,M., Marck,C., Sentenac,A. and Broach,J.R. (1992) Inactivation of the protein phosphatase 2A regulatory subunit A results in morphological and transcriptional defects in *S.cerevisiae*. *Mol. Cell. Biol.*, **12**, 4946–4959.

Welch,M.D., Holtzman,D.A. and Drubin,D.G. (1994) The yeast actin cytoskeleton. *Curr. Opin. Cell Biol.*, **6**, 110–119.

Received on January 10, 1995; revised on March 21, 1995